BMC Genomics

RESEARCH Open Access

Identification and core gene-mining of Weighted Gene Co-expression Network Analysis-based co-expression modules related to flood resistance in quinoa seedlings

Xuqin Wang[1†], Yutao Bai[1†], Lingyuan Zhang[1], Guofei Jiang[1], Ping Zhang[1], Junna Liu[1], Li Li[1], Liubin Huang[1] and Peng Qin[1*]

Abstract

Background As an emerging food crop with high nutritional value, quinoa has been favored by consumers in recent years; however, flooding, as an abiotic stress, seriously affects its growth and development. Currently, reports on the molecular mechanisms related to quinoa waterlogging stress responses are lacking; accordingly, the core genes related to these processes were explored via Weighted Gene Co-expression Network Analysis (WGCNA).

Results Based on the transcriptome data, WGCNA was used to construct a co-expression network of weighted genes associated with flooding resistance-associated physiological traits and metabolites. Here, 16 closely related co-expression modules were obtained, and 10 core genes with the highest association with the target traits were mined from the two modules. Functional annotations revealed the biological processes and metabolic pathways involved in waterlogging stress, and four candidates related to flooding resistance, specifically AP2/ERF, MYB, bHLH, and WRKY-family TFs, were also identified.

Conclusions These results provide clues to the identification of core genes for quinoa underlying quinoa waterlogging stress responses. This could ultimately provide a theoretical foundation for breeding new quinoa varieties with flooding tolerance.

Keywords WGCNA, Quinoa, Waterlogging stress, TFs

Background

Quinoa is a dicot herb of the amaranth family (Amaranthaceae) and Chenopodium genus and is one of the oldest crops in the Andean region of South America; moreover, it is known as a "false cereal crop" because of its cereal properties [1, 2]. Quinoa has an excellent amino acid composition and is cholesterol- and gluten-free [3] but contains a variety of biologically active substances, such as proteins, phenolic acids, flavonoids, and saponins, among others. These substances are important for promoting human health by lowering blood lipids or exerting antidiabetic and antioxidant effects, among others [4–6]. In addition, this crop can adapt to a wide range of ecological conditions and is highly tolerant to drought, cold, and frost [7].

Flooding is a common abiotic stressor, in which excessive precipitation or poor soil drainage leads to crop flooding, severely affecting plant physiological

†Xuqin Wang and Yutao Bai contributed equally to this work.

*Correspondence:
Peng Qin
wheat-quinoa@ynau.edu.cn
[1] College of Agronomy and Biotechnology, Yunnan Agricultural University, Kunming 650201, China

performance and yields [8]. Flooding reduces water absorption by plant root [9]saerobic respiration [10], and high-energy phosphorylated ATP [11], in addition to disrupting the structure of biofilms, mitochondria, and the internal structure of chloroplasts [12]. It also suppresses photosynthesis, transpiration, and stomatal conductance in plants [13], and the physiological and biochemical characteristics of plants are altered under waterlogging stress conditions. Jain et al. [14], in their study on the foliar application of nitrogen in response to waterlogging stress and its effects on sugarcane growth, found that the proline content was increased after flooding. Meanwhile, Thomas et al. [15] found that superoxide dismutase (SOD) and catalase activities were increased in soybean roots after flooding. Men et al. [16], in their study on the effect of waterlogging stress on the physiological characteristics of oilseed rape, found that the chlorophyll content and activities of antioxidant enzymes, such as peroxidase (POD), were elevated after flooding. Finally, Kumar et al. [17] found a decrease in soluble sugars in mung bean after flooding treatment. These results indicate that plants can regulate their physiological state in response to waterlogging stress.

A Weighted Gene Co-expression Network Analysis (WGCNA) is a tool used to identify the relationship between co-expression modules and traits, as well as highly relevant specific modules and core genes involved in plant growth and development [18]. It has also been widely used to mine pivotal genes in plants that are involved in the response to abiotic stresses. Zhang et al. [19] utilized quinoa WGCNA to identify core genes related to phosphorus levels in seedlings, finding two specific related modules and identifying 10 core genes. Moreover, Wang et al. [20] used WGCNA to identify hub genes related to heat stress responses in rice seedlings, and four modules were recognized. Yu et al. [21] identified and investigated 12 modules significantly associated with low temperature, after mining hub genes related to low-temperature responses in maize seedlings; they identified multiple hub genes associated with low-temperature stress from the four modules with the highest correlations. Further, Shen et al. [22] studied candidate genes related to heavy metal contents in the peel and pulp of ripe melons and identified five candidate related genes. However, there are fewer studies on the identification of core genes under waterlogging stress in quinoa. Based on WGCNA can identify gene collections with similar expression patterns, find out the links between gene collections and sample phenotypes, map the regulatory networks among genes and identify key regulatory genes. Meanwhile, it has been widely applied to other crops phased success. Therefore, in this study, we used Dianli-STZH (highly resistant), Dianli-60 (sensitive) and Yuncaili-2 (sensitive) as materials; and physiological indexes and significant accumulation of metabolites were made as correlation traits, and gene co-expression networks were generated and analyzed using WGCNA. In order to identify the coexpression modules closely related to flooding resistance and the core genes responding to waterlogging stress, and to provide valuable references and strong clues for the research of quinoa waterlogging stress.

Results

Quinoa physiological response to waterlogging stress

To study the physiological response of quinoa seedlings to waterlogging stress, SOD, POD, soluble sugars, soluble proteins, proline, and T-AOC physiological indices were determined. Under waterlogging stress, the soluble sugar content was significantly higher in all three plant material treatment groups, compared to that in the control group, and that in TR2 was significantly higher than that in TR1 and TR3 (Fig. 1A). Moreover, the content of soluble proteins in CR1 was significantly higher than that in TR1 for Dianli-STZH, whereas the content of soluble proteins in CR2 and CR3 was significantly lower than that in TR2 and TR3 (Fig. 1B). SOD and POD activities in the three lines showed different changes in the treatment and control groups; for example, the SOD activity in Dianli-STZH was higher than that in Dianli-60 and Yuncaili-2 and significantly lower than that in its own control group, whereas the SOD activities in CR2 and CR3 were significantly higher than those in the respective controls (Fig. 1C). POD activities in the three lines were all higher in the treatment groups than in the controls; here, TR2 had the lowest and TR1 had the highest POD activity (Fig. 1D). For Dianli-60, there was no significant difference in the proline content between treatment and control groups, but for Yuncaili-2, the proline content in CR3 was significantly higher than that in TR3, for Dianli-STZH the proline content in TR1 was significantly higher than that in CR1. In the treatment groups for the three materials, TR1 proline content was lowest, whereas that of TR3 was highest (Fig. 1E). Moreover, the T-AOC content in the treatment groups for the three materials was significantly higher than that in the controls, with the lowest T-AOC content observed in Yuncaili-2 and the highest in Dianli-60 (Fig. 1F). The lowest T-AOC content was found in Yuncaili-2 and the highest was in Dianli-60 (Fig. 1F).

Construction of weighted gene co-expression network

In total, 8630 genes were used to construct a weighted gene co-expression network after filtering genes with low expression. Cluster analysis was performed based on gene expression (Fig. 2), and there were no outlier

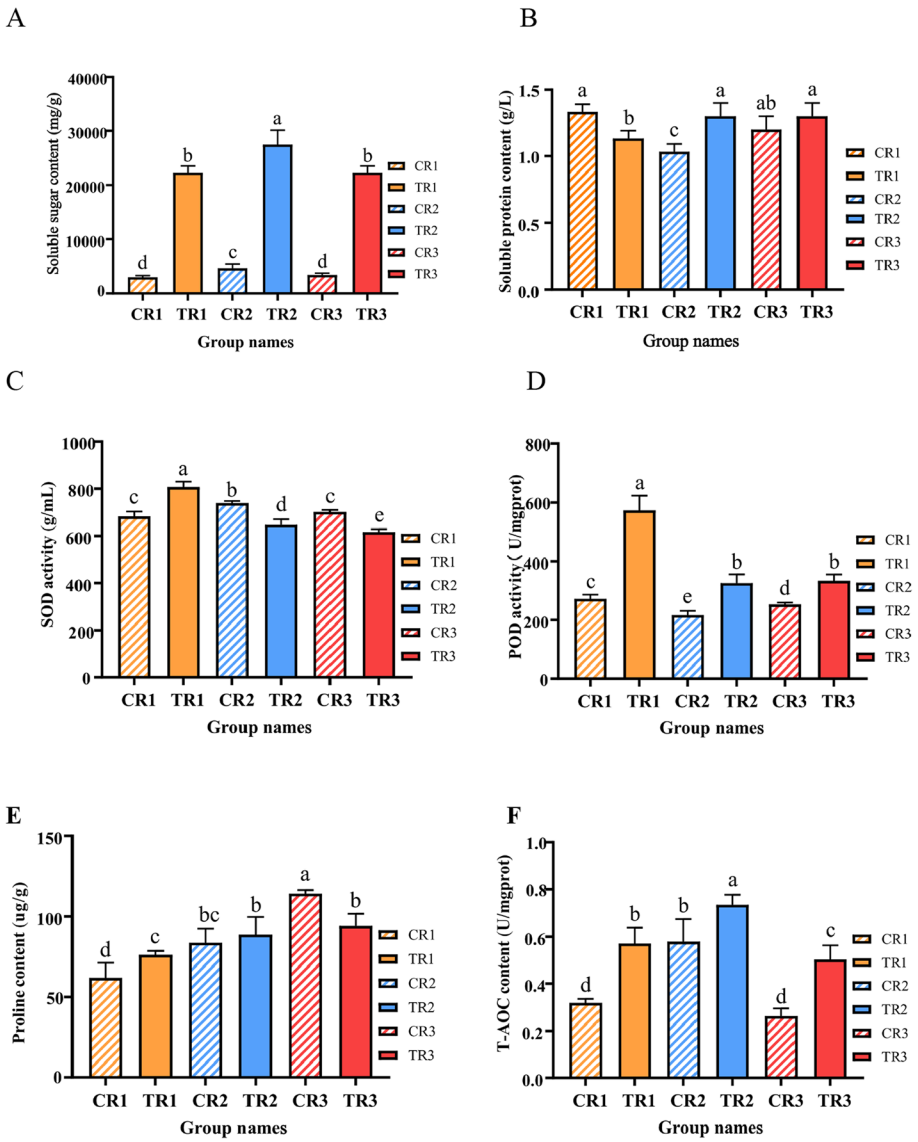

Fig. 1 Physiological changes in three quinoa seedling types under waterlogging stress. **A** soluble sugar content; (**B**) soluble protein content; (**C**) superoxide dismutase (SOD) activity; (**D**) peroxidase (POD) activity; (**E**) proline content; (**F**)Total antioxidant capacity (T-AOC) activity. Different letters (a-e) indicate significant differences ($P < 0.05$) and the same letter indicates no significance ($P > 0.05$)

samples. The pickSoftThreshold function was utilized to calculate a suitable soft threshold for the weighting coefficient, and the selection criteria for the soft threshold (i.e., to satisfy an R2 value close to 0.8, and at the same time to ensure a certain degree of gene connectivity). We selected a soft threshold of 12 to construct the co-expression network (Fig. 3). Subsequently, the dynamic cutting method was used to divide the network modules, and the small modules with high similarity were merged; finally, 16 modules were constructed (Fig. 4), with different colors indicating different modules.

Identification of specificity modules

Physiological indicators as trait data were correlated with the filtered genes, and a correlation heatmap was generated (Fig. 5A); in total, 16 modules were identified based on the correlation, among which the red module had the highest correlation coefficient with the soluble sugar content ($r = -0.75$, $p = 0.00033$), and it showed a high negative correlation with A, B, and CD indicators. Further, the purple module showed a highly significant positive correlation with POD ($r = 0.77$, $p = 0.00017$), indicating that the accumulation of purple module transcripts was associated with an increase in POD activity. Meanwhile,

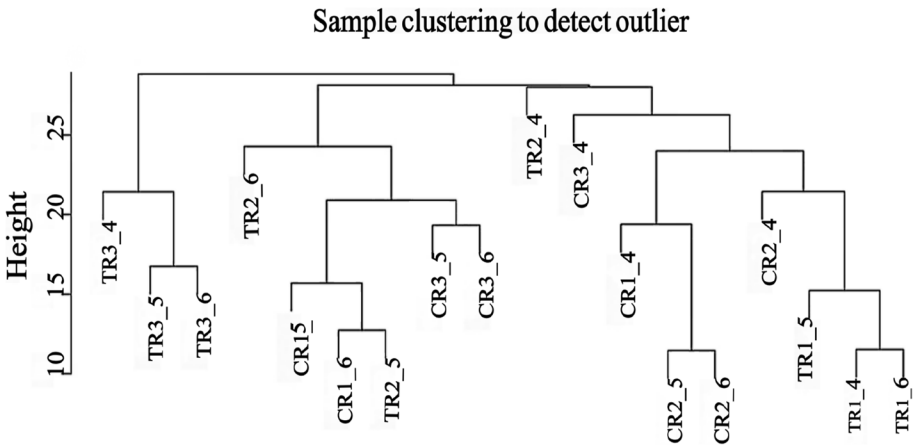

Fig. 2 Sample clustering diagram.The horizontal coordinate represents sample clustering, one column represents one sample, and the clustering is based on the similarity of gene expression between samples, the closer the gene expression between samples, the closer they are to each other

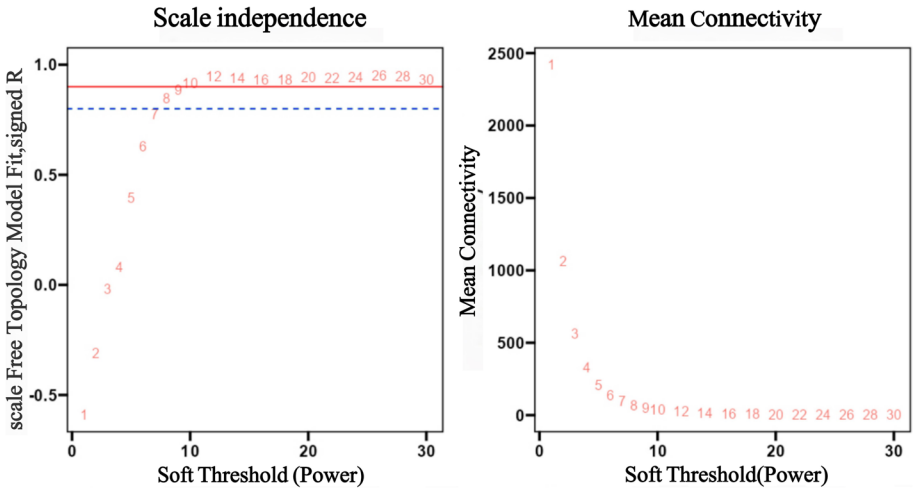

Fig. 3 Topology of quinoa seedling networks with different soft threshold powers.x-axis indicates the weight parameter β. y-axis in the left panel indicates the square of the correlation coefcient between log(k) and log(p(k)) in the corresponding network. The y-axis of the right panel represents the average of all gene adjacency functions in the corresponding gene module. The approximate scale-free topology is obtained at a soft threshold power of 12 for both genotypes

we screened the core genes (|MM|>0.8 and |GS|>0.6) in the purple module (Table S3), and we found that some of these core genes belonged to the *WRKY*, *HB-BELL*, *bHLH*, and *AP2/ERF-ERF* gene families.

After screening for differential metabolites with higher accumulation in each subgroup and noting that flavonoids were significantly accumulated in the treatment group, it was hypothesized that flavonoids have a potential role in coping with waterlogging stress. Therefore, the differentially accumulated flavonoids and genes were analyzed via WGCNA (Fig. 5B). Most of the flavonoid metabolites of the black module showed highly significant negative correlations ($P<0.001$), whereas most of the flavonoid metabolites of the brown module showed highly significant positive correlations, with pmp001288 (flavonoids) showing the highest and most significant correlation with the brown module ($P<0.001$). Finally, some of the core genes (|MM|>0.8 and |GS|>0.6) in the brown module were screened (Table S4), and some of these belonged to the *MYB*, *bHLH*, *Alfin-like*, and *GNAT* gene families. In total, four modules were constructed based on the correlations between the differential metabolite flavonoids and physiological indicators (Fig. 5C), with the highest correlation observed between POD and the brown module ($r=0.71$, $p=0.0009$), indicating that the accumulation of metabolites in the brown module was associated with elevated POD activity. Considering the high correlations among these data, we

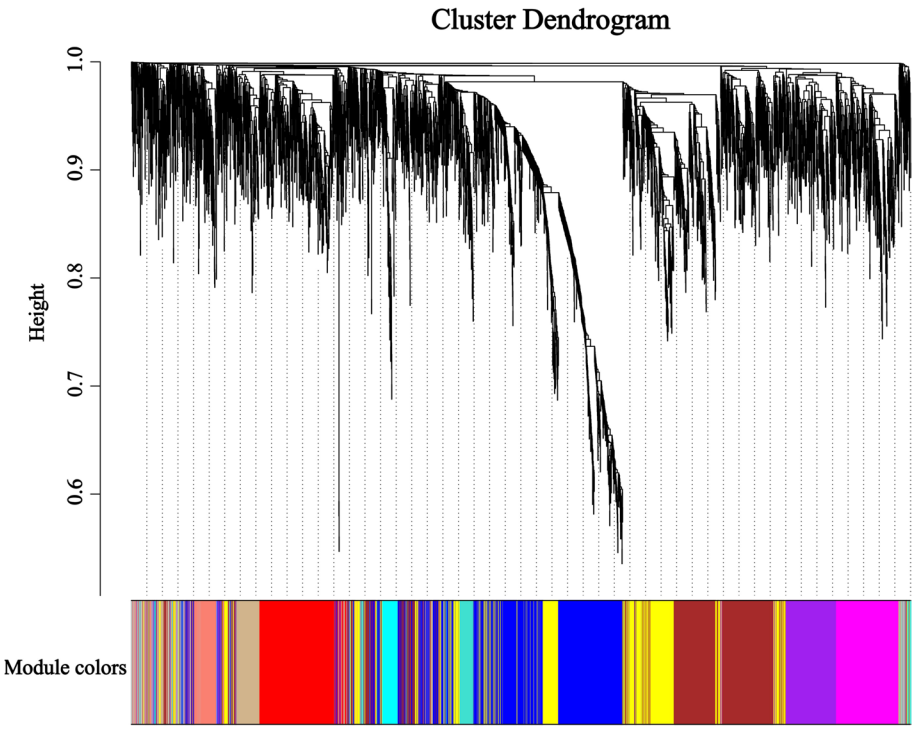

Fig. 4 gene clustering tree and division of modules. Gene tree maps obtained by color clustering dissimilarity of the corresponding modules based on consistent topological overlap and color row indications. Each row represents a color-coded module containing a set of highly linked genes

therefore analyzed the metabolites of the brown module (Table S5), which had a high percentage of flavonoids, amino acids and their derivatives, phenolic acids, and organic acids, suggesting that these substances might have a role in response to waterlogging stress. Finally, the purple and brown modules (metabolite-associated genes) were used for follow-up analyses to further explore their candidate genes.

Analysis of GO and KEGG enrichment for relevant specificity modules

To investigate the functional and metabolic classification of genes involved in the response to waterlogging stress, we conducted GO analysis all genes in the purple and brown modules, and the results are divided into three categories(Fig. 6A,B), namely biological processes (BPs), molecular functions (MFs), and cellular components (CCs). For genes in the purple module, BPs were mainly enriched in ionic homeostasis (GO:0050801) and inorganic ionic homeostasis (GO:0098771), MFs were mainly enriched in cysteine-type peptidase activity (GO:0008234) and drug transmembrane transporter protein activity (GO:0015238), and CCs were mainly enriched in the cytoplasmic vesicle fraction (GO:0044433), endosomal part (GO:0044440), and extracellular region part (GO:0044421) (Fig. 6C). For genes in the brown module, BPs were mainly enriched in the production of precursor metabolites and energy (GO:0006091) and in the processes of ribose phosphate metabolism (GO:0019693) and the metabolism of purine-containing compounds (GO:0072521), MFs were mainly enriched in the activity of oxidoreductases acting on NAD(P)H (GO:0016651) and threonine-type endopeptidase activity (GO:0004298), and CCs were mainly enriched in the mitochondrial inner membrane (GO:0005743), respiratory chain (GO:0070469), and mitochondrial protein complex (GO:0098798) (Fig. 6D). This suggests that flooding might trigger a response to waterlogging stress that is based on enzyme activities, signal transduction, and metabolic processes. These results also suggest that genes in the purple and brown modules that play important roles in the response to waterlogging stress are latent.

Annotating genes in the specificity module to the KEGG database provides insight into the primary functions of the genes in the module. KEGG enrichment analysis indicated that the genes in the purple module were mainly involved in metabolic pathways (ko01100), secondary metabolite biosynthesis (ko01110), purine metabolism (ko00230), and amino acid biosynthesis

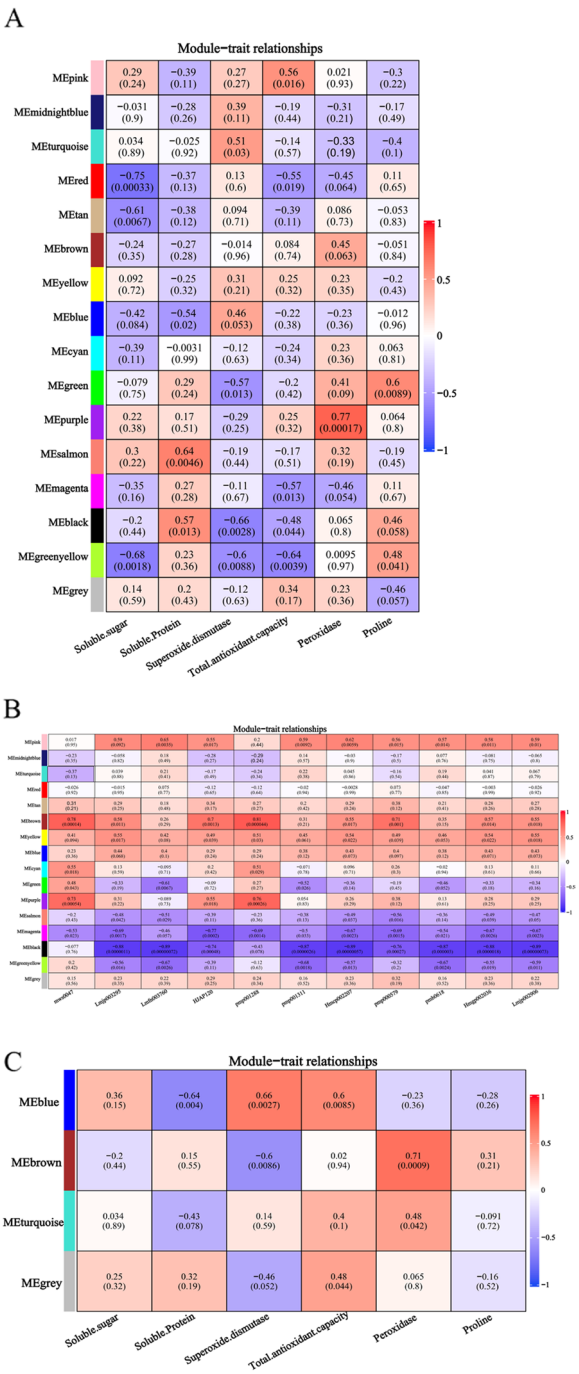

Fig. 5 Weighted correlation network analysis plots. **A** Heat map of gene co-expression network modules with physiological associations; **B** heat map of gene co-expression network with metabolite associations; C. metabolite co-expression network with physiological associations

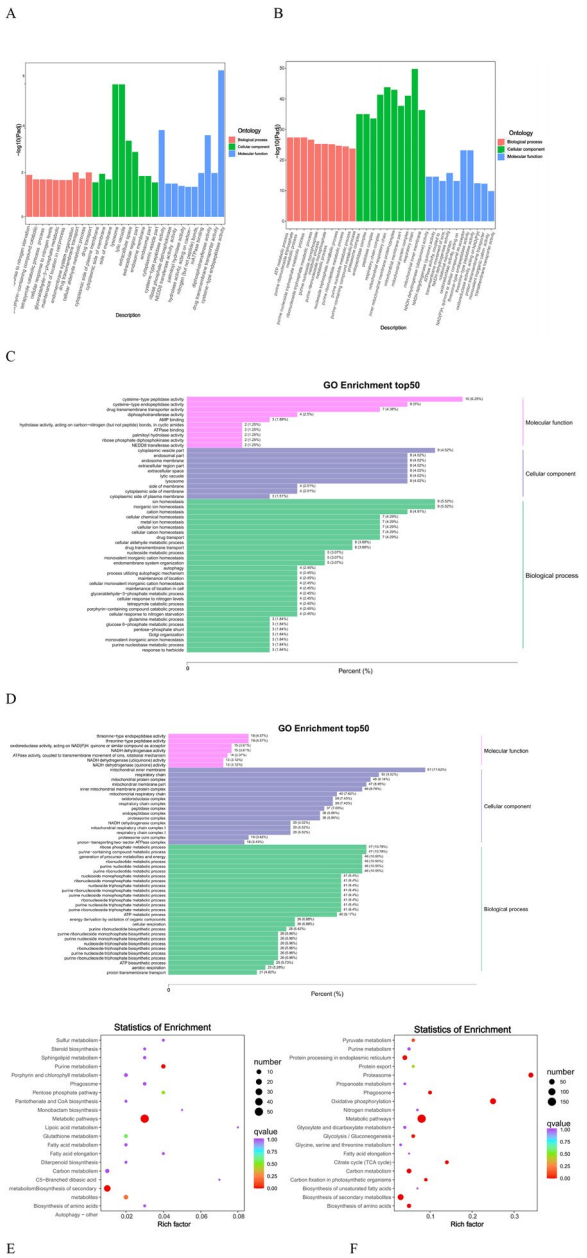

Fig. 6 Functional analysis of relevant specificity modules. Gene Ontology (GO) annotation (**A**, **B**), GO enrichment analysis (**C**, **D**), and Kyoto Encyclopedia of Genes and Genomes (KEGG) enrichment (**E**, **F**) analysis of candidate genes in purple (**A**, **C**, **E**) and brown (**B**, **D**, **F**) modules. x-axis of GO annotation shows GO terms for BP, CC and MF. y-axis shows the number of genes associated with GO terms. x-axis of GO enrichment shows the percentage of genes in GO terms and y-axis shows the percentage of genes in KEGG terms. The y-axis shows GO enrichment terms. x-axis for KEGG enrichment shows the percentage of genes in KEGG terms, and the y-axis shows KEGG enrichment terms

(ko01230) (Fig. 6E). Moreover, the genes in the brown module were mainly involved in protein processing in the endoplasmic reticulum (ko04141), the proteasome (ko03050), metabolic pathways (ko01100), oxidative phosphorylation (ko00190), the tricarboxylic acid cycle (ko00020), carbon metabolism (ko01200), glycolysis/glycolytic isomerization (ko00010), biosynthesis of secondary

metabolite synthesis (ko01110), and amino acid biosynthesis (ko01230) (Fig. 6F). This suggests that the genes in these modules might play key roles in the response of quinoa seedlings to waterlogging stress via alterations to metabolic pathways, biosynthesis, and energy metabolism.

Identification of core genes in the significant co-expression module associated with waterlogging stress in quinoa and construction of gene interaction network

Considering the high correlation between the aforementioned two modules and the associated shapes, combined with the GO and KEGG analysis results, it was speculated that they might have potential genes related to inundation stress. Therefore, these two modules were utilized to construct a gene interaction network and mine potential core genes. The genes with KME values in the top 20 were selected as preliminary candidate genes (Table S6), and the five core genes for each module were identified separately by calculating the BC using the cytoNCA plug-in in Cytoscape 3.9.1 software (Fig. 7 and Table 2). Through transcription factor identification, it was found that the core genes *LOC11068206* and *LOC110682343* in the purple module belong to the *WRKY* gene family, *LOC110682050* belongs to the *AP2*/*ERF* gene family, and *LOC110690303* and *LOC110687865* are structural genes. Moreover, in the brown module, it was determined that *LOC110681615* and *LOC110682220* belong to the *MYB* gene family, *LOC110681724* belongs to the *bHLH* gene family, and *LOC110683180* and *LOC110688261* belong to structural genes in the brown module. In addition, we performed promoter analysis of structural genes (Table S6) and found that 39 structural genes have homeostatic elements that bind to the MYB family of transcription factors, of which four structural genes have MYB-binding sites involved in the regulation of flavonoid biosynthesis genes, 15 have MYB-binding sites involved in the response to light, and 20 have MYB-binding sites involved in the drought-inducible sites.

Transcription factors activated under waterlogging stress

To understand the expression of transcription factors in response to waterlogging stress, Table S7 shows the top 10 transcription factors in terms of numbers; these were mainly concentrated in the *AP2/ERF, bHLH, WRKY, NAC, MYB, FAR1*, and *C3H* families, with the coding genes with the highest numbers being *FAR1* and *bHLH*. Of note, the most highly expressed genes belonged to the *MYB*, *bZIP*, *AP2*/*ERF-ERF*, and *bHLH* families; seven of the top 30 expressed genes belonged to the *AP2*/*ERF* family of transcription factors, and the expression of genes in flood-resistant varieties was significantly higher than that in sensitive varieties. Because the *AP2/ERF* family of transcription factors has been reported to confer resistance to waterlogging in maize (*ZmEREB180*), rice (*OsSub1A*), and *Arabidopsis* (*AtRAP2.2 and AtERF72*), we used these genes to identify motifs based on the screened *AP2/ERF* family core gene *LOC110682050*(Fig. 8A). Five motifs were identified from five *AP2/ERF*-encoding genes, and *LOC110682050* was determined to share three motifs with them, with all of the genes encoding proteins with AP2 domains. We therefore suspect that the mechanism

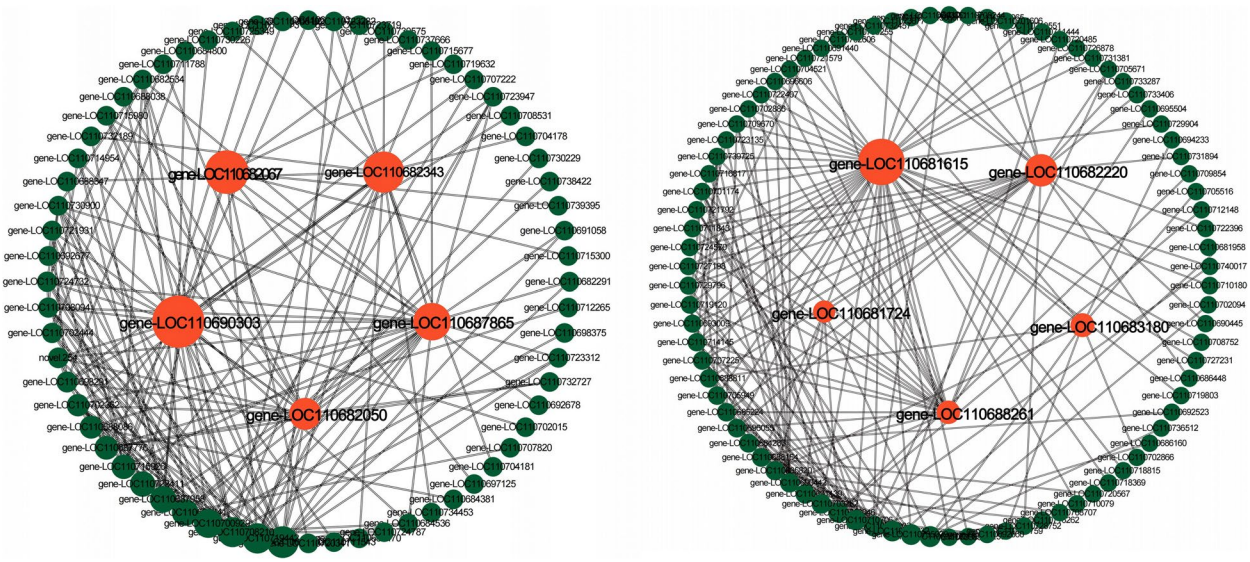

Fig. 7 Candidate hub genes for purple (**A**) and brown (**B**) modules obtained from the interaction network analysis of known core genes. Orange color represents the screened core genes, and larger dots represent larger BC values

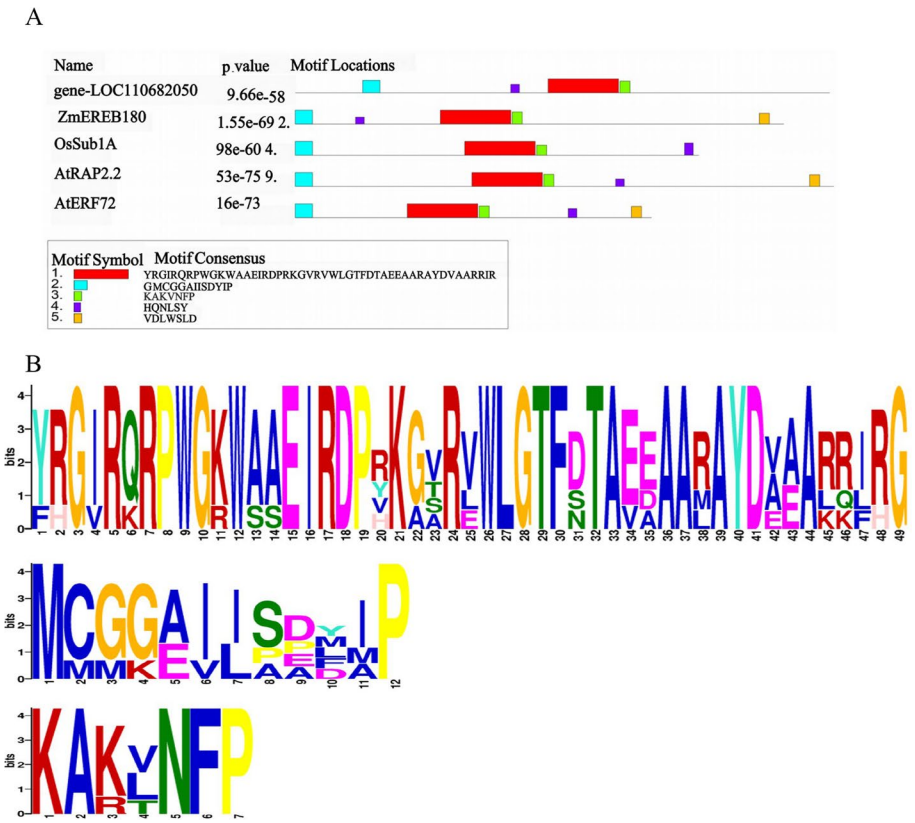

Fig. 8 Comparative analysis of the five genes of the AP2/ERF family. **A** Structural domain analysis. **B** Conserved structural domain sequence tags

underlying the response to waterlogging stress is related to the expression of transcription factors, especially with respect to ethylene signaling.

Real-time fluorescence quantitative PCR validation

Ten the core genes for real-time fluorescence quantitative PCR, and three replicates were set up for each reaction. $2-\Delta\Delta$Ctwas used to analyze the normalized expression of each sample, so as to calculate $2-\Delta\Delta$Ct and SD, and the FPKM and SD of the validation genes were also calculated. based on the $2-\Delta\Delta$Ct of the validation genes and the FPKM of the sequenced genes, the results showed that the expression trends detected by RT-qPCR matched well with the RNAseq data, which proved the reliability of core gene expression (Fig. 9A-J and Tables 1 and 2).

Discussion

Quinoa, as an emerging pseudocereal crop, has attracted much attention in recent years; however, flooding severely affects its growth and development. Plant roots are injured under waterlogging stress, leading to changes in plant physiology and metabolism that affect plant growth [23]. However, osmoregulation, as a mechanism of defense against adversity and stress, can reduce cellular water potential and ensure normal plant growth [24], and the increase in osmoregulatory substances (soluble sugars, proline, and soluble proteins) can be used to cope with waterlogging stress in plants [25]. Barickman et al. [8] found elevated proline levels and differences in soluble sugar contents in cucumbers under waterlogging stress. Fante et al. [26] also found an increase in the soluble sugar content in the leaves of soybean after flooding. This is in general agreement with the results of the present study. Because we found that the soluble sugar content of quinoa seedlings after flooding was significantly higher in the treated group than in the control group and the proline content was significantly higher in the highly resistant materials after waterlogging stress, it was speculated that quinoa could respond to waterlogging stress by regulating the contents of osmotic substances after flooding, thus improving resistance to flooding. Flooding reduces reactive oxygen species in plants, which in turn disrupts the redox balance and causes damage to plant growth [27]. To reduce the damage caused to plants, plants produce many ROS-scavenging enzymes, such as POD and SOD. In a previous study, Zhang et al. [28] found that after flooding, the damage to barley was reduced through an increase in antioxidant enzyme

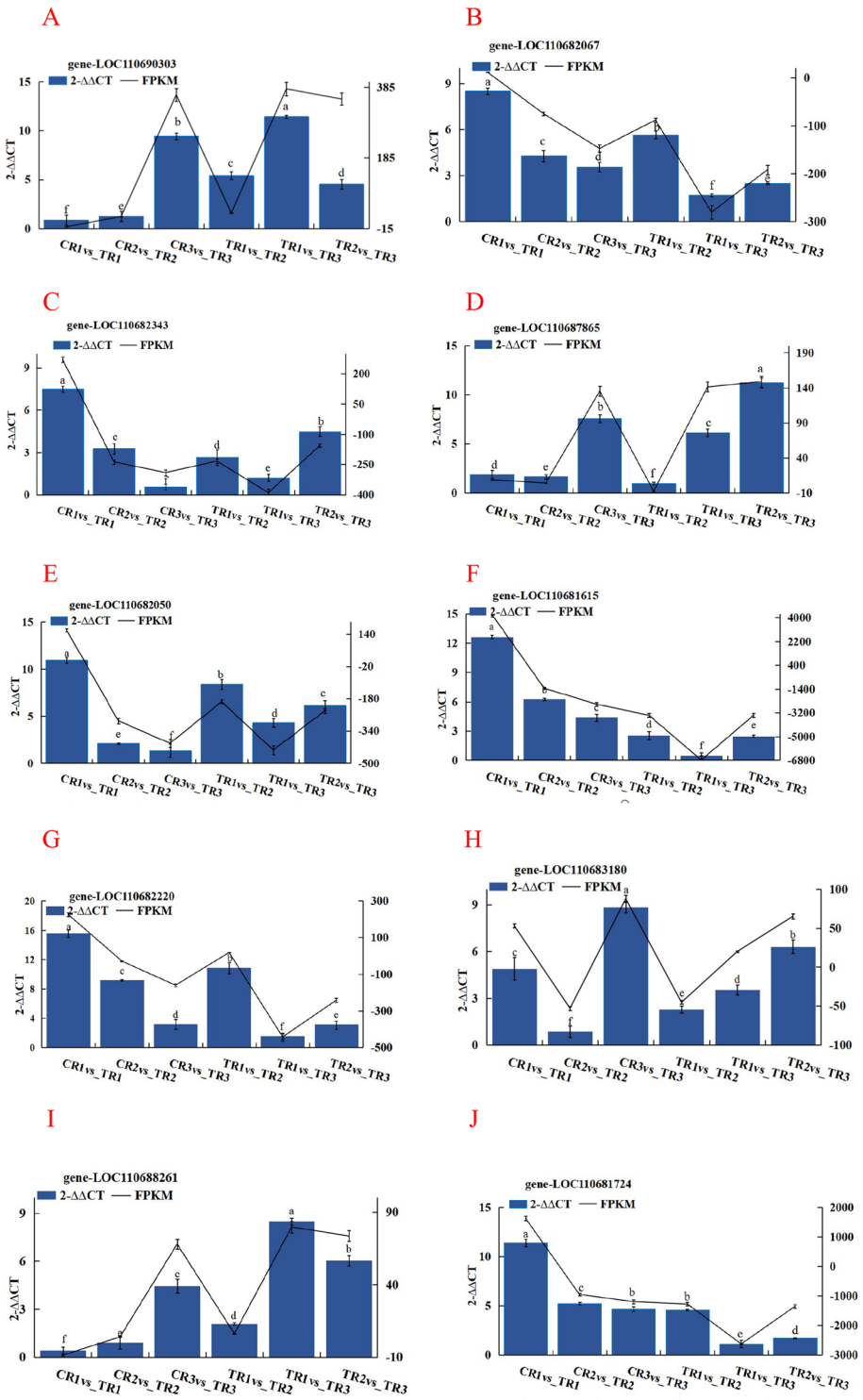

Fig. 9 (A-J) Validation of gene expression levels of core genes by RT-qPCR

activities. Moreover, Zhu et al. [29] obtained the same conclusion using grapes, where the antioxidant enzyme activities of SOD and POD were elevated in the leaves after flooding. In this study, we also found that the POD and SOD enzyme activities of quinoa seedlings were significantly higher under waterlogging stress than under

Table 1 Functional annotation of core genes in the waterlogging stress-related specificity module

Module	Module candidate hub genes	Transcription factor family	Gene function
Purple	gene-LOC110690303	-	Early nodular protein-like protein 2
	gene-LOC110682067	WRKY family protein	Possible WRKY transcription factor 13, which regulates flowering time, is involved in adversity stress
	gene-LOC110682343	WRKY family protein	Possible WRKY transcription factor 15 that regulates plant growth and salt/osmotic stress responses
	gene-LOC110687865	-	Histone B-like protease 2
	gene-LOC110682050	ERF family protein	Ethylene-responsive transcription factor ERF113-like, transcriptional activator involved in the regulation of plant development and tolerance to abiotic stress, acts as a positive regulator of tolerance to Waterlogging stress. Delaying flooding-induced premature senescence by regulating stomatal closure and antioxidant enzyme activities
Brown	gene-LOC110681615	MYB family protein	The transcription factor MYB35, a positive regulator of abscisic acid (ABA) responses, causes growth arrest during seed germination and is involved in the regulation of leaf morphogenesis and pollen grain development
	gene-LOC110682220	MYB family protein	The transcription factor, MYB16-like, is highly expressed in roots and at lower levels in stems and flowers
	gene-LOC110683180	-	ATP synthase subunit d, mitochondria
	gene-LOC110688261	-	Peptidyl-prolinyl cis–trans isomerase CYP20-1-like
	gene-LOC110681724	bHLH family protein	Transcription factor bHLH18-like, symbiotic interactions with endophytes of the Sebacinaceae family of fungi, transcriptional activators that regulate the expression of NAI2, PYK10, and PBP1, mediate the formation of endoplasmic reticulum bodies

Table 2 Primer sequences to validate genes

Quantity	gene-ID	NCBI-Gene ID	Primer	5′ to 3′
1	gene-LOC110690303	110,690,303	Forward Primer	TTTATCGTCTTTGCCTTT
			Reverse Primer	CTTGCCTACCATTAACAT
2	gene-LOC110682067	110,682,067	Forward Primer	TGTAGAGTGAAGAAGAGA
			Reverse Primer	CAGAAGAAGTTGTTAAGC
3	gene-LOC110682343	110,682,343	Forward Primer	ATCTTCTTCAAACCTCTC
			Reverse Primer	CACTCTCCATATTACTATTATC
4	gene-LOC110687865	110,687,865	Forward Primer	AGAGTGAGAAGAGGAATA
			Reverse Primer	ATAGTGCTACATTGAGAC
5	gene-LOC110682050	110,682,050	Forward Primer	ATTGAAGAAGAAGAAGGAA
			Reverse Primer	ACCACAGGCTATAATAATC
6	gene-LOC110681615	110,681,615	Forward Primer	GTGTTGTTGGTTCTTATAC
			Reverse Primer	TTGTTCTGTTGAGTTGAT
7	gene-LOC110682220	110,682,220	Forward Primer	TACCAAGGATAACAACAAT
			Reverse Primer	ACTAACCAAACTAATACCAT
8	gene-LOC110683180	10,683,180	Forward Primer	AAGAAGCAGAACAACAAT
			Reverse Primer	ATAGTCATTGCGAATCTC
9	gene-LOC110688261	110,688,261	Forward Primer	TATCACAACCGTAACAAC
			Reverse Primer	GTCAGCAATAACAACCTT
10	gene-LOC110681724	110,681,724	Forward Primer	TTCCAATCATTCCTTGTC
			Reverse Primer	CGTTATCGTTATCATTACTG
Internal reference gene	TUB-6	831,100	Forward Primer	TGAGAACGCAGATGAGTGTATG
			Reverse Primer	GAAACGAAGACAGCAAGTGACA

control conditions. This suggests that the increase in antioxidant enzyme activities under waterlogging stress results in free radical scavenging to cope with waterlogging stress, as the growth status of the highly resistant varieties in this study was significantly better than that of the sensitive varieties.

Metabolites comprise the hub of genes and phenotypes, and plants can be studied based on a combination of metabolites and physiological changes [30]. A WGCNA of metabolites with physiological indices revealed that the core metabolites under waterlogging stress were flavonoids, organic acids, and phenolic acids. Xuan et al. [31] found that phenolic acids are involved in the response to waterlogging stress through improvements in the antioxidant capacity of rice seedlings. Meanwhile, Wang et al. [32] revealed that waterlogging stress significantly increases the total flavonoid content and affects secondary metabolic biosynthesis in Chrysanthemum officinale. Further, the results of promoter analysis also showed that many structural genes have cis-acting elements that bind to the *MYB* family of transcription factors, and some of these structural genes also have *MYB*-binding sites involved in the regulation of flavonoid biosynthesis genes, which indirectly suggests that flavonoids might be regulated by the *MYB* family and play an important role in the response to flooding stress. An analysis of the relevant specificity modules identified using WGCNA revealed that these differential genes were mainly enriched in ribose phosphate metabolism, the metabolism of purine-containing compounds, protein processing in the endoplasmic reticulum, carbon metabolism, glycolysis/glycolysis, and amino acid biosynthesis. Guo et al. [33] found that quinoa responds to waterlogging stress mainly through sugars, as well as alcohols, and Zhu et al. [29] identified differentially regulated genes associated with amino acid and sugar metabolism that can reduce the damage to grapes in response to waterlogging stress, which is similar to our differential gene enrichment results under flooding conditions. Regarding the grape flooding response, differentially expressed genes associated with amino acid and sugar metabolism were found to be activated to reduce damage under waterlogging stress, which is similar to our differential gene enrichment results under flooding conditions.

Most of the subsequent core genes screened encoded members of the *WRKY, MYB, AP2/ERE*, and *bHLH* transcription factor families, which have been shown to have important roles in waterlogging stress [34]. For example, *AP2/EREBP* and *MYB* are significantly expressed and increase plant tolerance under waterlogging stress [35, 36]. Moreover, Zhao et al. [37] found the significant upregulation of *ERF, bHLH,* and *MYB* family expression in sensitive and flood-tolerant *Chrysanthemum* varieties. Our core gene annotation results revealed that these proteins are mainly encoded by *AP2*/*ERE*, *bHLH*, and *MYB*, which is in general agreement with previous studies on transcription factors involved in the flooding response under waterlogging stress. The core genes *LOC110682067* and *LOC110682343* encode proteins of the WRKY transcription factor family. Meng et al. [38] found that some *WRKY* genes are involved in the waterlogging stress response. Further, Campbell et al. [39] reported upregulation of the expression of *WRKY* transcription factors after 24, 48, and 72 h of submergence, and Viana et al. [40] also demonstrated that under waterlogging stress, *WRKY* transcription factors can regulate the development of aeration tissues in rice. *LOC110682050* belongs to the *AP2/ERF* family of transcription factors, and *AP2/ERF* has a key role in the ethylene response, which can broadly regulate the response of plants to adversity and stress. Du et al. [41] analyzed 20 *ERF-B2* subfamily genes in the maize genome under waterlogging stress and found that nine of them were responsive to waterlogging stress. Wang et al. [42] also found that *ERF* transcription factors are involved in the flooding-response process in sesame. *LOC110681615* and *LOC110682220* belong to the *MYB* gene family, which plays an important role in regulating plant development, metabolism, and abiotic stress tolerance [36]. Zhang et al. [28] found that in *Arabidopsis thaliana*, the transcription factor *MYB30* represses the synthesis of ethylene through 1-aminocyclopropane-1-carboxylic acid synthetase 7, which is then involved in the response to waterlogging stress. Similarly, Owusu et al. [43] found that the *MYB* transcription factor gene in cotton is highly sensitive to flooding under waterlogging stress. These results suggest that the core genes that we identified also play important roles in the response of quinoa to waterlogging stress.

Conclusion

In this study, we found that quinoa responds to waterlogging stress through the regulation of antioxidant enzyme (SOD, POD) activities, the soluble sugar content, and the accumulation of flavonoids and phenolic acids. Moreover, WGCNA identified two key modules, and 10 core genes involved in response to inundation stress, mainly belonging to the *WRKY*, *AP2*/*ERF*, *MYB* and *bHLH* gene families, were identified. Through functional annotation, some of the core genes were found to be closely related to the reported abiotic stress regulatory pathways, among which the core genes encoded by

AP2/ERF were highly homologous to different reported genes that are involved in the response to inundation stress. The results of this study could provide clues for further studies on the search for core genes underlying flooding resistance in quinoa and also provide theoretical support for the breeding of new quinoa varieties with flooding tolerance.

Materials and methods

Material planting and growth conditions

The high-generation cultivars Dianli-STZH, Dianli-60, and Yuncaili-2, which were independently selected and bred by Yunnan Agricultural University, were planted in a glass greenhouse at the Modern Agricultural Education and Research Base of Yunnan Agricultural University, Xundian County, Kunming (E 102°41′, N 25°20′, Kunming, China). Uniform seeds were selected and hole-sown in 50-hole seedling trays (54 cm × 28 cm × 12 cm) to ensure 2–3 seedlings per hole, and six trays were planted for each material and divided into treatment and control groups. During the growth period, the average temperature was 23.6℃ and the sunshine duration was approximately 10 h. When the seedlings reached 6–8 true leaves, the treatment group was flooded by submerging the seedling trays in water, and the water surface was always kept at approximately 1–2 cm above the soil surface, whereas the control group was subjected to normal cultivation management. A previous study showed that after 240 h of flooding treatment, for the sensitive materials, the biggest morphological difference between the control and treated groups was related to the phenomenon of rigidity, and leaf yellowing was extremely serious; however, the highly resistant materials always maintained normal growth [33](Fig. 10). The greatest phenotypic differences between the treatment groups and the control were observed at this stage, and therefore, 240 h was determined to be the optimal sampling time in this study, at which time the aboveground parts of the three quinoa lines were sampled. For three biological replicates, with 18 samples in total, the specimens were flash frozen in liquid nitrogen at stored at − 80℃. Sample information is shown in Table 3:

Measurement of physiological and biochemical indicators

The soluble sugar content was determined based on the method of Kim et al. [44]; antioxidant enzymes (POD,SOD) were assessed according to the method of Tang et al. [45]. The soluble protein content was determined through staining [46], and the proline content was determined referring to the method of Elasad et al. [47]. Finally, T-AOC determination was performed according to the instructions of the kit (colorimetric method), which was obtained from Nanjing Jianjian Biological Engineering Research Institute Co. (Nanjing, China).

Data acquisition

Eighteen samples were sent to Wuhan Metware Biotechnology Co. Ltd. (www.metware) for transcriptome and metabolome assays. The transcriptome analysis process included RNA extraction, detection, and library construction. RNA extraction was performed using the

Table 3 Sample information

Sample	Treaments	CK
Dianli-STZH	TR1	CR1
Dianli-60	TR2	CR2
Yuncaili-2	TR3	CR3

Fig. 10 Morphological map of the three materials after 240 h of flooding treatment. Dianli-STZH (**A**), Dianli-60 (**B**), and Yuncaili-2 (**C**), where the top of the picture is the treatment and the bottom is the control

method of Zeng et al. [48], and it was analyzed using agarose gel electrophoresis to determine RNA integrity and the presence of DNA contamination. The RNA concentration was accurately determined using a Qubit 2.0 fluorometer, and the integrity of the detected RNA was analyzed using an Agilent 2100 Bioanalyzer. Library construction was accomplished using the method of Zhu et al. [29]. After sequencing was completed, the available clean data were analyzed, and gene annotations were performed using Tophat2 (v2.1.0) software [49]. After annotation, the results were compared and counts were enumerated using RSEM [50] to compare the number of reads in the samples and transcripts; the FPKM (fragments per kilobase of exon model per million mapped fragments) [49] conversion was used to determine the expression levels of transcripts and genes. Metabolite extraction was performed using the method of Chen et al. [51]. Characterization of the metabolites was performed using secondary spectral information from the MWDB (Metware Database), and quantitative analysis of the metabolites was performed using the multiple reaction monitoring mode of triple quadrupole mass spectrometry. Metabolites were further analyzed using orthogonal partial least squares discrimination and multivariate statistical analysis with supervised pattern recognition to screen for differential metabolites with a VIP value > 1 and fold-change ≥ 2 or ≤ 0.5 [52].

Construction of weighted gene co-expression network

Gene co-expression networks were constructed using the WGCNA (version 1.6.1) package in R software [18]. The expression profile matrices of the genes were derived from the gene expression in all samples. Genes with an FPKM value less than 10 were filtered out, and those remaining were used for WGCNA. To make the network conform to the scale-free network distribution, the pickSoftThreashold computational weights were chosen to have a value of power of 12, and the blockwiseModules were utilized to construct the scale-free network, with the parameters set according to the default settings. The metabolomic abundance data of physiological indicators and flavonoids were used as the associated traits (Table S1), which were correlated with the filtered 8,630 genes (Table S2). Then, the core genes were categorized into 16 modules using WGCNA, and the correlation of each module with the trait was calculated; a higher correlation coefficient was indicative of a higher the correlation between the module and the trait, whereas a lower correlation coefficient was indicated of a lower correlation.

Screening specificity modules and GO (Gene Ontology) and KEGG (Kyoto Encyclopedia of Genes and Genomes) functional enrichment analysis

The correlation coefficients (r-values) and corresponding p-values between the eigenvectors (module eigengene) of each module and the different traits were calculated separately to determine the specificity of modules. Modules with an |r| value > 0.7 and $p < 0.01$ were selected as specific modules, and these were analyzed via KEGG and GO analyses. GO and KEGG enrichment analyses were performed using the clusterProfile package in the R program [21], with corrections based on multiple hypothesis testing, with a corrected $p < 0.05$ considered significantly enriched.

Screening core genes for specific modules and construction of gene interaction networks

The connectivity of a gene in a module represents the regulatory relationship between that gene and other genes, and it reflects the role of the gene in the module; higher connectivity indicates a stronger regulatory role for the gene in the module and a potential core gene [53].Therefore, the first 20 genes were initially screened as candidate core genes by calculating the KME (module eigengene-based connectivity) value within the module, and the core genes were subsequently screened by calculating the BC (betweenness) value using the cytonca plugin in Cytoscape 3.9.1 software [54]. In conjunction with promoter analysis, structural gene promoter regions (2,000 bp upstream) were identified, cis-acting element information was obtained, and gene interaction network maps were generated with reference to Wang et al. [55].

Transcription factor identification analysis

Transcription factor families were identified and annotated using ITAK (IAITAM, Canton, OH, USA) software [56, 57]. The core genes were subjected to protein sequence extraction using the NCBI website, and blast were selected from the plantTFDB database [58] for transcription factor analysis and prediction to obtain transcription factor families in each module and to further understand the functions of the core genes. The conservation of core genes was predicted using the motif-inspired Multiple Expectation Maximization (MEME, http:// meme-suite.org/tools/meme) tool [59].

Real-time fluorescence quantitative PCR validation

To verify the reliability of gene expression, all samples of the ten core genes were selected and three biological replicates were set up for RT-qPCR verification.The primers for the related genes used for RT-qPCR analysis were designed in Beacon Designer7.9.and the TUB-6

Table 4 Reaction system and conditions for qPCR 20 μL

Component	Volume(uL)
2 × Perfectstarttm SYBR qPCR Supermix	10
Calibration Solution	0.4
Nuclease-free Water (RNase free water)	6.8
Forward Primer(10 μM)	0.4
Reverse Primer(10 μM)	0.4
cDNA(200 μg/μL)	2
Total volume	20

gene was selected as the internal reference gene. Then RT-qPCR was performed using PerfectStart SYBR qPCR Supermix (TransGen Biotech, Beijing, China).the reaction volume was 20 uL (Table 3), and the thermal cycling conditions were set to 94℃ (30 s), 94℃ (5 s), 60℃ (30 s), and 40 cycles, and finally, the reaction volume was 20 uL (Table 4). $2-\Delta\Delta Ct$ method to calculate the relative gene expression levels [60].

Abbreviations

BC	Betweenness
TF	Transcription factors
WGCNA	Weighted gene co-expression network analysis
ME	Module eigengene
GS	Gene Signifcance
MM	Module Membership
KME	Module gene-based connectivity
VIP	Variable importance in the projection
GO	Gene Ontology
KEGG	Kyoto Encyclopedia of Genes and Genomes

Supplementary Information

The online version contains supplementary material available at https://doi.org/10.1186/s12864-024-10638-y.

Supplementary Material 1.
Supplementary Material 2.
Supplementary Material 3.
Supplementary Material 4.
Supplementary Material 5.
Supplementary Material 6.
Supplementary Material 7.
Supplementary Material 8.

Acknowledgements
We wish to acknowledge the Wuhan Metware Biotechnology Co., Ltd., for Professional technical services. We would like to thank Editage (www.editage.cn) for English language editing. We also thank professor Peng Qin conducted with the experiments for their valuable help and guidance.
XQW wrote the original draft ,carried out the formal analysis and performed the methodology. YTB wrote the original draft and carried out the formal analysis. LYZ did the conceptualization, and wrote, reviewed, and edited the manuscript. GFJ carried out the formal analysis, performed the methodology, and visualized the data. PZ collected the field samples and prepared the plant materials. JNL carried out the formal analysis and investigated the data. LL and LBH carried out the formal analysis and investigated the data. PQ supervised the data and carried out the project administration and funding acquisition. All authors contributed to the article and approved the submitted version.

Authors' contributions
XQW wrote the original draft ,carried out the formal analysis and performed the methodology. YTB wrote the original draft and carried out the formal analysis. LYZ did the conceptualization, and wrote, reviewed, and edited the manuscript. GFJ carried out the formal analysis, performed the methodology, and visualized the data. PZ collected the field samples and prepared the plant materials. JNL carried out the formal analysis and investigated the data. LL and LBH carried out the formal analysis and investigated the data. PQ supervised the data and carried out the project administration and funding acquisition. All authors contributed to the article and approved the submitted version.

Funding
We gratefully acknowledge the financial support of the Yunnan Expert Workstation (202205AF150001) and the "Xingdian Talent"Industry Innovation Talent Program in Yunnan Province (XDYC CYCX-2022–0031).

Availability of data and materials
The original contributions presented in the study are publicly available. This data can be found here National Center for BiotechnologyInformation (NCBI) SRA database under accession number SRP383884.We hereby declare that the materials used in this study (Dianli-STZH, Dianli-60、Yuncaili-2) were independently selected and bred by Qin Peng's group at Yunnan Agricultural University and have the right to use them.

Declarations

Ethics approval and consent to participate
The study complies with relevant institutional, national, and international guidelines and legislations. All procedures were conducted in accordance with the guidelines. We hereby declare that the materials used in this study (Dianli-STZH, Dianli-60、Yuncaili-2) were independently selected and bred by Qin Peng's group at Yunnan Agricultural University and have the right to use them. In this study, stable quinoa lines independently selected by Yunnan Agricultural University were used as materials, and named Dianli-STZH, Dianli-60、Yuncaili-2 by Professor Qin Peng. The lines of quinoa seeds are cultivars, not wild. Quinoa seeds are collected with permission in accordance with institutional and national guidelines. The collection of quinoa lines is in line with institutional and national guidelines.

Consent for publication
Not applicable.

Competing interests
The authors declare no competing interests.

Received: 5 May 2024 Accepted: 19 July 2024
Published online: 29 July 2024

References

1. Carciochi RA, Galvan-D'Alessandro L, Vandendriessche P, Chollet S. Effect of Germination and Fermentation Process on the Antioxidant Compounds of Quinoa Seeds. Plant Foods Hum Nutr. 2016;71(4):361–7.
2. Vega-Galvez A, Miranda M, Vergara J, Uribe E, Puente L, Martinez EA. Nutrition facts and functional potential of quinoa (Chenopodium quinoa willd.), an ancient Andean grain: a review. J Sci Food Agric. 2010;90(15):2541–7.
3. Filho AM, Pirozi MR, Borges JT, Pinheiro SH, Chaves JB, Coimbra JS. Quinoa: Nutritional, functional, and antinutritional aspects. Crit Rev Food Sci Nutr. 2017;57(8):1618–30.
4. Cao Y, Zou L, Li W, Song Y, Zhao G, Hu Y. Dietary quinoa (Chenopodium quinoa Will.) polysaccharides ameliorate high-fat diet-induced hyperlipidemia and modulate gut microbiota. INT J BIOL MACROMOL. 2020;163:55–65.

5. Mudgil P, Kilari BP, Kamal H, Olalere OA, FitzGerald RJ, Gan C, Maqsood S. Multifunctional bioactive peptides derived from quinoa protein hydrolysates: Inhibition of α-glucosidase, dipeptidyl peptidase-IV and angiotensin I converting enzymes. J CEREAL SCI. 2020;96: 103130.
6. Daliri H, Ahmadi R, Pezeshki A, Hamishehkar H, Mohammadi M, Beyrami H, Khakbaz Heshmati M, Ghorbani M. Quinoa bioactive protein hydrolysate produced by pancreatin enzyme- functional and antioxidant properties. LWT. 2021;150: 111853.
7. Ruiz KB, Biondi S, Oses R, Acuña-Rodríguez IS, Antognoni F, Martinez-Mosqueira EA, Coulibaly A, Canahua-Murillo A, Pinto M, Zurita-Silva A, et al. Quinoa biodiversity and sustainability for food security under climate change. A review AGRON SUSTAIN DEV. 2014;34(2):349–59.
8. Barickman TC, Simpson CR, Sams CE. Waterlogging Causes Early Modification in the Physiological Performance, Carotenoids, Chlorophylls, Proline, and Soluble Sugars of Cucumber Plants. Plants (Basel). 2019;8(6):160.
9. Tournaire-Roux C, Sutka M, Javot H, Gout E, Gerbeau P, Luu DT, Bligny R, Maurel C. Cytosolic pH regulates root water transport during anoxic stress through gating of aquaporins. NATURE. 2003;425(6956):393–7.
10. Zhou W, Chen F, Meng Y, Chandrasekaran U, Luo X, Yang W. Shu K Plant waterlogging/flooding stress responses. From seed germination to maturation. Plant Physiol Biochem. 2020;148:228–36.
11. Gibbs J, Greenway H. Review. Mechanisms of anoxia tolerance in plants I. Growth, survival and anaerobic catabolism. Funt Plant Biol. 2003;30(1):1–47.
12. Ren B, Zhang J, Dong S, Liu P, Zhao B. Effects of Waterlogging on Leaf Mesophyll Cell Ultrastructure and Photosynthetic Characteristics of Summer Maize. PLOS ONE. 2016;11(9): e161424.
13. Saddiq MS, Wang X, Iqbal S, Hafeez MB, Khan S, Raza A, Iqbal J, Maqbool MM, Fiaz S, Qazi MA, et al. Effect of Water Stress on Grain Yield and Physiological Characters of Quinoa Genotypes. In Agronomy. 2021;11(10):1934.
14. Jain R, Singh SP, Singh A, Singh S, Chandra A, Solomon S. Response of Foliar Application of Nitrogen Compounds on Sugarcane Grown Under Waterlogging Stress. SUGAR TECH. 2016;18(4):433–6.
15. Thomas AL, Guerreiro SM, Sodek L. Aerenchyma formation and recovery from hypoxia of the flooded root system of nodulated soybean. Ann Bot. 2005;96(7):1191–8.
16. Men S, Chen H, Chen S, Zheng S, Shen X, Wang C, Yang Z, Liu D. Effects of supplemental nitrogen application on physiological characteristics, dry matter and nitrogen accumulation of winter rapeseed (*Brassica napus L.*) under waterlogging stress. Sci Rep. 2020;10(1):10201.
17. Kumar P, Pal M, Joshi R, Sairam RK. Yield, growth and physiological responses of mung bean [*Vigna radiata (L.*) Wilczek] genotypes to waterlogging at vegetative stage. Physiol Mol Biol Pla. 2013;19(2):209–20.
18. Zong J, Chen P, Luo Q, Gao J, Qin R, Wu C, Lv Q, Zhao T, Fu Y. Transcriptome-Based WGCNA Analysis Reveals the Mechanism of Drought Resistance Differences in Sweetpotato (Ipomoea batatas (L.) Lam.). Int J Mol Sci. 2023;24(18):14398.
19. Zhang S, Liu J, Shi L, Wang Q, Zhang P, Wang H, Liu J, Li H, Li L, Li X, et al. Identification of core genes associated with different phosphorus levels in quinoa seedlings by weighted gene co-expression network analysis. BMC GENOMICS. 2023;24(1):399.
20. Wang Y, Chen S, Yu O. Metabolic engineering of flavonoids in plants and microorganisms. Appl Microbiol Biotechnol. 2011;91(4):949–56.
21. Yu T, Zhang J, Cao J, Ma X, Li W, Yang G. Hub Gene Mining and Co-Expression Network Construction of Low-Temperature Response in Maize of Seedling by WGCNA. Genes (Basel). 2023;14(8):1598.
22. Shen Q, Wu X, Tao Y, Yan G, Wang X, Cao S, Wang C, He W. Mining Candidate Genes Related to Heavy Metals in Mature Melon (*Cucumis melo L.*) Peel and Pulp Using WGCNA. Genes (Basel). 2022;13(10):1767.
23. Ahmed S, Nawata E, Hosokawa M, Domae Y, Sakuratani T. Alterations in photosynthesis and some antioxidant enzymatic activities of mungbean subjected to waterlogging. Plant Sci. 2002;163(1):117–23.
24. Ozturk M, Turkyilmaz UB, Garcia-Caparros P, Khursheed A, Gul A, Hasanuzzaman M. Osmoregulation and its actions during the drought stress in plants. Physiol Plant. 2021;172(2):1321–35.
25. Kreuzwieser J, Rennenberg H. Molecular and physiological responses of trees to waterlogging stress. PLANT CELL ENVIRON. 2014;37(10):2245–59.
26. Fante CA, Alves JD, Goulart PDFP, Deuner S, Silveira NM. Respostas fisiológicas em cultivares de soja submetidas ao alagamento em diferentes estádios. BRAGANTIA. 2010;69:253–61.
27. Gill SS, Tuteja N. Reactive oxygen species and antioxidant machinery in abiotic stress tolerance in crop plants. Plant Physiol Biochem. 2010;48(12):909–30.
28. Zhang Y, Xie Y, Shi H, Zhuang Y, Zheng Y, Lin H, Zhou H. MYB30 Regulates Submergence Tolerance by Repressing Ethylene Biosynthesis via ACS7 in Arabidopsis. PLANT CELL PHYSIOL. 2023;64(7):814–25.
29. Zhu X, Li X, Jiu S, Zhang K, Wang C, Fang J. Analysis of the regulation networks in grapevine reveals response to waterlogging stress and candidate gene-marker selection for damage severity. R Soc Open Sci. 2018;5(6): 172253.
30. Gao J, Ren R, Wei Y, Jin J, Ahmad S, Lu C, Wu J, Zheng C, Yang F, Zhu G. Comparative Metabolomic Analysis Reveals Distinct Flavonoid Biosynthesis Regulation for Leaf Color Development of Cymbidium sinense "Red Sun." INT J MOL SCI. 2020;21(5):1869.
31. Xuan TD, Khang DT. Effects of Exogenous Application of Protocatechuic Acid and Vanillic Acid to Chlorophylls, Phenolics and Antioxidant Enzymes of Rice (*Oryza sativa L.*) in Submergence. Molecules. 2018;23(3):620.
32. Wang T, Zou Q, Guo Q, Yang F, Wu L, Zhang W. Widely Targeted Metabolomics Analysis Reveals the Effect of Flooding Stress on the Synthesis of Flavonoids in Chrysanthemum morifolium. Molecules. 2019;24(20):369.
33. Guo Y, Wang Q, Zhang H, Huang T, Zhang X, Xie H, Liu J, Zhang P, Li L, Qin P. Responses to waterlogging stress in quinoa seedlings based on metabolomic and transcriptomic analysis. Environ Exp Bot. 2022;203: 105044.
34. Borrego-Benjumea A, Carter A, Tucker JR, Yao Z, Xu W, Badea A. Genome-Wide Analysis of Gene Expression Provides New Insights into Waterlogging Responses in Barley (*Hordeum vulgare L.*). Plants (Basel). 2020;9(2):240.
35. Dietz KJ, Vogel MO, Viehhauser A. AP2/EREBP transcription factors are part of gene regulatory networks and integrate metabolic, hormonal and environmental signals in stress acclimation and retrograde signalling. PROTOPLASMA. 2010;245(1–4):3–14.
36. Dubos C, Stracke R, Grotewold E, Weisshaar B, Martin C, Lepiniec L. MYB transcription factors in Arabidopsis. TRENDS PLANT SCI. 2010;15(10):573–81.
37. Zhao N, Li C, Yan Y, Cao W, Song A, Wang H, Chen S, Jiang J, Chen F. Comparative Transcriptome Analysis of Waterlogging-Sensitive and Waterlogging-Tolerant Chrysanthemum morifolium Cultivars under Waterlogging Stress and Reoxygenation Conditions. INT J MOL SCI. 2018;19(5):1455.
38. Meng D, Li Y, Bai Y, Li M, Cheng L. Genome-wide identification and characterization of WRKY transcriptional factor family in apple and analysis of their responses to waterlogging and drought stress. Plant Physiol Biochem. 2016;103:71–83.
39. Campbell MT, Proctor CA, Dou Y, Schmitz AJ, Phansak P, Kruger GR, Zhang C, Walia H. Genetic and molecular characterization of submergence response identifies Subtol6 as a major submergence tolerance locus in maize. PLOS ONE. 2015;10(3): e120385.
40. Viana VE, Marini N, Busanello C, Pegoraro C, Fernando JA, Da Maia LC, Costa De Oliveira A. Regulation of rice responses to submergence by WRKY transcription factors. Biol Plantarum. 2018;62(3):551–5602.
41. Du H, Huang M, Zhang Z, Cheng S. Genome-wide analysis of the AP2/ERF gene family in maize waterlogging stress response. EUPHYTICA. 2014;198:115–26.
42. Wang L, Dossa K, You J, Zhang Y, Li D, Zhou R, Yu J, Wei X, Zhu X, Jiang S, et al. High-resolution temporal transcriptome sequencing unravels ERF and WRKY as the master players in the regulatory networks underlying sesame responses to waterlogging and recovery. GENOMICS. 2021;113(1 Pt 1):276–90.
43. Owusu AG, Lv YP, Liu M, Wu Y, Li CL, Guo N, Li DH, Gao JS. Transcriptomic and metabolomic analyses reveal the potential mechanism of waterlogging resistance in cotton (*Gossypium hirsutum L.*). Front Plant Sci. 2023;14:1088537.
44. Kim SW, Lee SK, Jeong HJ, An G, Jeon JS, Jung KH. Crosstalk between diurnal rhythm and water stress reveals an altered primary carbon flux into soluble sugars in drought-treated rice leaves. Sci Rep. 2017;7(1):8214.
45. Tang Y, Li J, Song Q, Cheng Q, Tan Q, Zhou Q, Nong Z, Lv P. Transcriptome and WGCNA reveal hub genes in sugarcane tiller seedlings in response to drought stress. Sci Rep. 2023;13(1):12823.

46. Lin T, Zhou R, Bi B, Song L, Chai M, Wang Q, Song G. Analysis of a radiation-induced dwarf mutant of a warm-season turf grass reveals potential mechanisms involved in the dwarfing mutant. Sci Rep. 2020;10(1):18913.
47. Elasad M, Ahmad A, Wang H, Ma L, Yu S, Wei H. Overexpression of CDSP32 (GhTRX134) Cotton Gene Enhances Drought, Salt, and Oxidative Stress Tolerance in Arabidopsis. Plants (Basel). 2020;9(10):1388.
48. Zeng Z, Zhang S, Li W, Chen B, Li W. Gene-coexpression network analysis identifies specific modules and hub genes related to cold stress in rice. BMC GENOMICS. 2022;23(1):251.
49. Trapnell C, Pachter L, Salzberg SL. TopHat: discovering splice junctions with RNA-Seq. BIOINFORMATICS. 2009;25(9):1105–11.
50. Li B, Dewey CNRSEM. accurate transcript quantification from RNA-Seq data with or without a reference genome. BMC BIOINFORMATICS. 2011;12:323.
51. Chen W, Gong L, Guo Z, Wang W, Zhang H, Liu X, Yu S, Xiong L, Luo J. A novel integrated method for large-scale detection, identification, and quantification of widely targeted metabolites: application in the study of rice metabolomics. MOL PLANT. 2013;6(6):1769–80.
52. Thevenot EA, Roux A, Xu Y, Ezan E, Junot C. Analysis of the Human Adult Urinary Metabolome Variations with Age, Body Mass Index and Gender by Implementing a Comprehensive Workflow for Univariate and OPLS Statistical Analyses. J PROTEOME RES. 2015;14(8):3322–35.
53. Zhang G, Tanakamaru K, Abe J, Morita S. Influence of waterlogging on some anti-oxidative enzymatic activities of two barley genotypes differing in anoxia tolerance. ACTA PHYSIOL PLANT. 2007;29(2):171–6.
54. Shannon P, Markiel A, Ozier O, Baliga NS, Wang JT, Ramage D, Amin N, Schwikowski B, Ideker T. Cytoscape: a software environment for integrated models of biomolecular interaction networks. GENOME RES. 2003;13(11):2498–504.
55. Wang R, Shu P, Zhang C, Zhang J, Chen Y, Zhang Y, Du K, Xie Y, Li M, Ma T, et al. Integrative analyses of metabolome and genome-wide transcriptome reveal the regulatory network governing flavor formation in kiwifruit (Actinidia chinensis). Newphytol. 2022;233(1):373–89.
56. Jin J, Zhang H, Kong L, Gao G, Luo J. PlantTFDB 30: a portal for the functional and evolutionary study of plant transcription factors. Nucleic Acids Res. 2014;42(D1):1182-D1187.
57. Perez-Rodriguez P, Riano-Pachon DM, Correa LG, Rensing SA, Kersten B, Mueller-Roeber B. PlnTFDB: updated content and new features of the plant transcription factor database. Nucleic Acids Res. 2010;38(Database issue):D822–7.
58. Jin J, Tian F, Yang DC, Meng YQ, Kong L, Luo J, Gao G. PlantTFDB 40: toward a central hub for transcription factors and regulatory interactions in plants. Nucleic Acids Res. 2017;45(D1):D1040-1045.
59. Bailey TL, Elkan C. Fitting a mixture model by expectation maximization to discover motifs in biopolymers. Proc Int Conf Intell Syst Mol Biol. 1994;2:28–36.
60. Livak KJ, Schmittgen TD. Analysis of relative gene expression data using real-time quantitative PCR and the $2^{-\Delta\Delta CT}$ Method. Methods. 2001;25:402–8.

Publisher's Note